Journal of Materials and Environmental Sciences
ISSN : 2028-2508
CODEN : JMESCN

J. Mater. Environ. Sci., 2018, Volume 9, Issue 11, Page 3026-3034

http://www.jmaterenvironsci.com

Hydroxycarboxylic acids as corrosion inhibitors on aluminium metal: a computational study

A. M. Ayuba[1*], A. Uzairu[2], H. Abba[2], G. A. Shallangwa[2]

1. Department of Pure and Industrial Chemistry, Bayero University, Kano, Nigeria.
2. Department of Chemistry, Ahmadu Bello University, Zaria, Kaduna, Nigeria

Received 31 Dec 2018,
Revised 13 Jan 2019,
Accepted 15 Jan 2019

Keywords
- ✓ *Adsorption,*
- ✓ Aluminium,
- ✓ Computation,
- ✓ Corrosion,
- ✓ Inhibitors.

ayubaabdullahi@buk.edu.ng
Phone: +2348062771500;

Abstract

Corrosion inhibition mechanism of three hydroxycarboxylic acids including tartaric, citric and malic acids on aluminium (1 1 0) surface was investigated by quantum chemical calculation and molecular dynamics simulation. Quantum chemical parameters such as E_{HOMO}, E_{LUMO}, energy gap (ΔE), dipole moment (μ), electronegativity (χ), global hardness (η) and fraction of electron transfers from the inhibitor molecule to the aluminium surface (ΔN) have been studied to investigate their relative corrosion inhibition performances. Local reactive sites parameters of the studied molecules have been analyzed through Fukui indices. Moreover, adsorption behaviour of the inhibitor molecules on Al (1 1 0) surface have also been analyzed using molecular dynamics simulation. The binding strength of the concerned inhibitor molecules on aluminium surface follows the order citric acid>malic acid>tartaric acid which is in good agreement with the experimentally determined inhibition efficiencies. In view of the above, our approach will be helpful for quick Quantum chemical calculations and Molecular dynamics simulation prediction of a potential inhibitor from a lot of similar inhibitors and subsequently in their rational designed synthesis for corrosion inhibition application following a wet chemical synthetic route.

1. Introduction

Aluminium metal has a great technological importance owing to its low cost, light weight, and high thermal and electrical conductivity [1-2]. The most important feature of aluminium is its corrosion resistance due to the formation of a protective film on its surface upon its exposure to the atmosphere or water [3-4]. The protection of aluminum and its oxide films against the corrosive action of chloride ions has been extensively investigated and a great number of inhibitors have been studied [4-9].

Experimental means are useful to explain the inhibition mechanism but they are often expensive and time-consuming. Ongoing hardware and software advances have opened the door for powerful use of theoretical chemistry in corrosion inhibition research. Several quantum chemical methods and molecular modeling techniques have been performed to correlate the inhibition efficiency of the inhibitors with their molecular properties [10-20]. In many cases the parameters connected with the electronic and the chemical structure of the molecule act simultaneously on the inhibitor efficiency and it is difficult to decide which parameter plays the most important role in increasing the inhibitor efficiency [21-24]. For this reason organic compounds, which have similar structures were chosen in this investigation. It is assumed that in this way, the influence of the chemical structure will be very similar and the influence of the electronic structure will be better investigated. Despite the large number of organic compounds, there is always a need for developing new organic corrosion inhibitors [25-27]. The adsorption of the organic inhibitors on the aluminum surface can markedly change the corrosion-resisting property of it [28], and so the study of the relations between the adsorption and corrosion

inhibition is of great importance. Adsorption characteristics of these inhibitors depend on several factors including the nature and number of potential adsorption sites present in the inhibitor molecule. Numerous attempts are made to link the corrosion inhibitor efficiency with a number of structural parameters of these molecules [29-35]. The choice of these compounds is based on molecular structure considerations, i.e. these are organic substances with almost similar chemical structure, and the differences in the inhibition properties should be mainly due to the difference in electronic structure of these compounds.

This purpose of the present work is to study the inhibition efficiency of the chosen hydroxycarboxylic acids and correlate their efficiency with the quantum chemical parameters of the investigated compounds. The calculated quantum chemical parameters are the highest occupied molecular orbital (E_{HOMO}), the lowest occupied molecular orbital (E_{LUMO}), the separation energy (ΔE), the dipole moment (μ), and those parameters that give valuable information about the reactive behaviour such as the electronegativity (χ), the ionization potential (I), the hardness (η), the softness (σ), and the fraction of electrons transferred from the inhibitor to the metal surface (ΔN). Furthermore, the interaction energies of the investigated inhibitors on the aluminum surface were also studied to discuss the inhibition mechanism.

2. Theoretical Modeling and Simulation Methods

All theoretical calculations were performed using the density functional theory (DFT) electronic structure programs Forcite and DMol3 as contained in the Materials Studio 7.0 software (Accelrys, Inc.). There is no doubt that the recent progress in DFT has provided a very useful tool for understanding molecular properties and for describing the behaviour of atoms in molecules [17-18, 25, 33-35]. DFT methods have become very popular in the last decade due to their accuracy and shorter computational time. DFT has been found to be successful in providing insights into chemical reactivity and selectivity, in terms of global parameters such as electronegativity (χ), hardness (η), and softness (σ), and local ones such as the Fukui function f(r) and local softness s(r). Thus, for an N-electron system with total electronic energy E and an external potential v(r), the chemical potential μ, known as the negative of the electronegativity χ, has been defined as the first derivative of E with respect to N at constant v(r) as in equation (1)[2, 4, 8-9, 17-20, 26, 31-35]:

$$\chi = -\mu = -\left(\frac{\partial E}{\partial N}\right)_{v(r)} \quad \text{.....(1)}$$

Hardness (η) has been defined within DFT as the second derivative of E with respect to N at constant v(r) as in equation (2)[17-20, 26-27, 31-35]:

$$\eta = \left(\frac{\partial^2 E}{\partial N^2}\right)_{v(r)} = \left(\frac{\partial \mu}{\partial N}\right)_{v(r)} \quad \text{.....(2)}$$

The number of electrons transferred (ΔN) from the inhibitor molecule to the aluminium metal surface was calculated by using equation (3) [28,31-35]:

$$\Delta N = \frac{\chi_{Al} - \chi_{Inh}}{2(\eta_{Al} + \eta_{Inh})} \quad \text{.....(3)}$$

where χ_{Al} and χ_{inh} denote the absolute electronegativity of aluminium and the inhibitor molecule, respectively, and η_{Al} and η_{inh} denote the absolute hardness of aluminium and the inhibitor molecule, respectively. Electron affinity (I) and ionization potential (A) are related in turn to the energy of the highest occupied molecular orbital (E_{HOMO}) and of the lowest unoccupied molecular orbital (E_{LUMO}) using the equations (4) and (5) [2, 4, 8-9, 17-20, 29, 31-36]:

$$I = -E_{HOMO} \quad \text{.....(4)}$$

$$A = -E_{LUMO} \quad \text{.....(5)}$$

These quantities are related to the electron affinity (A) and ionization potential (I) using equations (6) and (7) :

$$\chi = \left(\frac{I + A}{2}\right) = -\frac{E_{LUMO} + E_{HOMO}}{2} \quad \text{.....(6)}$$

$$\eta = \left(\frac{I - A}{2}\right) = -\frac{E_{LUMO} - E_{HOMO}}{2} \quad \text{.....(7)}$$

Global softness can also be defined in equation (8) as [2, 4, 8-9, 29, 31, 32, 36]:

$$\sigma = \frac{1}{\eta} \quad \text{.....(8)}$$

The local reactivity of the inhibitor molecule was analyzed through evaluation of the Fukui indices [30]. The Fukui indices are measures of chemical reactivity, as well as an indicative of the reactive regions and the nucleophilic and electrophilic behaviour of the molecule. Regions of a molecule where the Fukui function is large are chemically softer than regions where the Fukui function is small, and by invoking the hard and soft acids and bases (HSAB) principle in a local sense, one may establish the behaviour of the different sites with respect to hard or soft reagents. The Fukui function f(r) is defined as the first derivative of the electronic density q(r) with respect to the number of electrons N at constant external potential v(r). Thus, using a scheme of finite difference approximations from Mulliken population analysis of atoms in the hydroxycarboxylic acids molecules and depending on the direction of electron transfer, we have equations (9), (10), (11) [4, 8-9, 30, 36]:

For nucleophilic attack: $f_k^+ = q_k(N+1) - q_k(N)$ .....(9)

$f_k^- = q_k(N) - q_k(N-1)$ .....(10) For electrophilic attack:

For radical attack: $$f_k^0 = \frac{q_k(N+1) - q_k(N-1)}{2} \quad \text{.....(11)}$$

where q_k is the gross charge of atom k in the molecule, i.e., the electron density at a point r in space around the molecule. N corresponds to the number of electrons in the molecule. N + 1 corresponds to an anion, with an electron added to the LUMO of the neutral molecule; N - 1 corresponds to the cation with an electron removed from the HOMO of the neutral molecule. All calculations were done at the ground state geometry. These functions were condensed to the nuclei by using an atomic charge partitioning scheme, such as Mulliken population analysis in equations (9-11).

Molecular dynamics (MD) simulation of the interaction between a single molecule and the Al surface was performed using Forcite quench MD in Material Studio (MS) Modeling 7.0 software to sample many different low-energy minima and to determine the global energy minimum [4, 35-37]. Calculations were carried out in a 9 x 7 supercell using the condensed-phase optimized molecular potentials for atomistic simulation studies (COMPASS) force field and the Smart algorithm. Of the many kinds of Al surfaces, Al (1 1 0) is the most densely packed and also the most stable [4, 35-36, 38]. The Al crystal was cleaved along the (1 1 0) plane. The Al slab built for the docking process was significantly larger than the inhibitor molecules in order to avoid edge effects during docking. Temperature was fixed at 350 K, with NVE ensemble, with time step of 1 fs and simulation time of 5 ps. The system was quenched every 250 steps with the Al (1 1 0) surface atoms constrained. Optimized structure of the inhibitor molecule was used for the simulation. Adsorption of a single hydroxycarboxylic acid molecule onto the Al (1 1 0) surface provides access to the adsorption energetics and its effect on the inhibition efficiency of molecule. Thus, the adsorption energy, E_{ads}, between the hydroxycarboxylic acid molecule and Al (1 1 0) surface was calculated using equation (12) [4, 35-36,38]:

$Energy_{Adsorption} = E_{Complex} - (E_{Inhibitor} + E_{Alsurface})$ .....(12)

where $E_{complex}$ is the total energy of the Al surface and inhibitor, E_{Al} is the energy of the Al surface without the inhibitor, and $E_{inhibitor}$ is the energy of the inhibitor without the Al surface.

The 2D and 3D structures of the selected amino/hydroxycarboxylic acids are as presented in Figure (1):

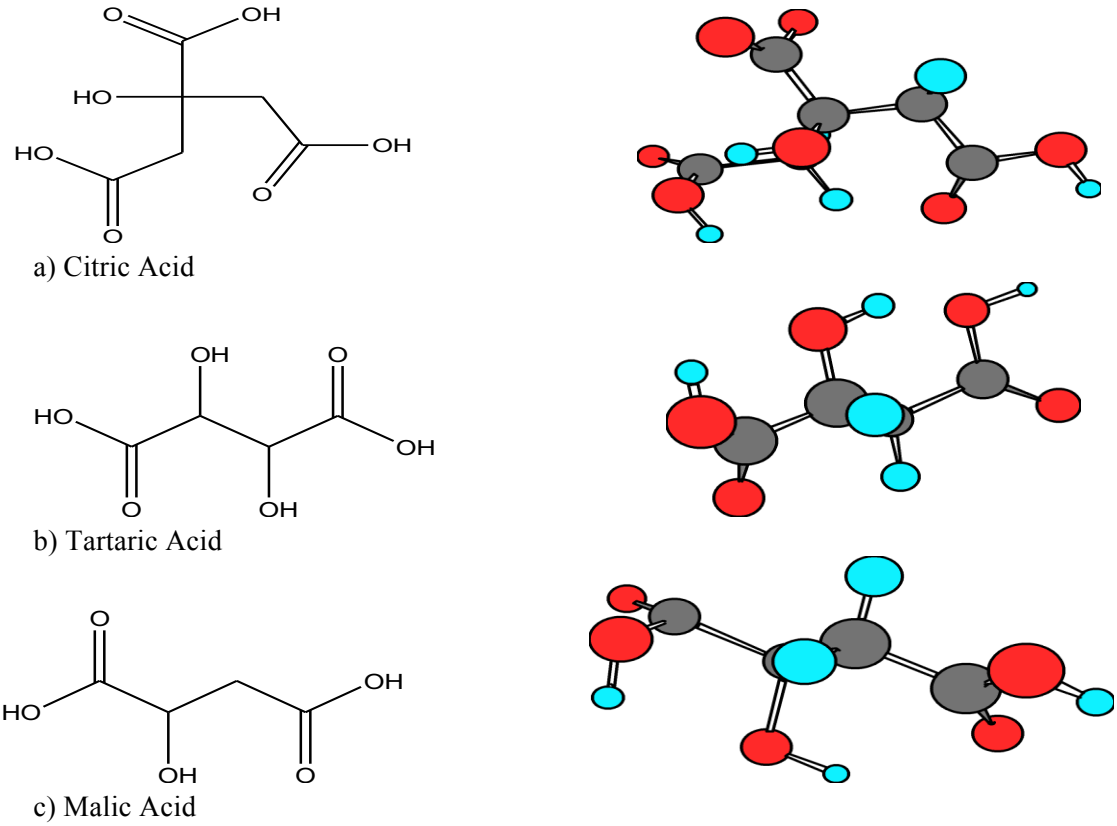

Figure 1: Chemical structures of hydroxycarboxylic acids: (a) Citric Acid (b) Tartaric Acid (c) Malic Acid

3. Results and discussion

Calculations were performed to describe the electronic structures of the molecules of the hydroxycarboxylic acids with a view to establish the active sites as well as local reactivity of the molecules. Simulations were performed by means of the DFT electronic structure program DMol3 using a Mulliken population analysis [39-41]. Electronic parameters for the simulation include unrestricted spin polarization using the DND basis set and the Perdew–Wang (PW) local correlation density functional. Figures 2, 3, 4 illustrates the optimized structure, highest occupied molecular orbital (HOMO), and lowest unoccupied molecular orbital (LUMO) of tartaric, citric and malic acids respectively. The electron density is saturated all around each molecule which should facilitate flat-lying adsorption orientations.

The regions of high HOMO density are the sites at which electrophiles attack and represent the active centers, with the utmost ability to bond to the metal surface, whereas the LUMO orbital can accept the electrons in the d-orbital of the metal using antibonding orbitals to form feedback bonds [41-43]. The numerical values of the HOMO (E_{HOMO}) and LUMO (E_{LUMO}) as well as the energy gap $\Delta E = E_{LUMO-HOMO}$ are presented in Table 1, together with some other quantum chemical parameters related to the molecular electronic structure of the most stable conformation of the molecules. High values of E_{HOMO} indicate the disposition of the molecule to donate electrons to an appropriate acceptor with vacant molecular orbitals, whereas low values of ΔE will favor good inhibition efficiencies because the energy to remove an electron from the last occupied orbital will be minimized [41, 44-46]. The obtained values show that the molecules all have comparable E_{HOMO} values, which is not very surprising because the functional groups that comprise the HOMO are identical for all the molecules. The similarities in quantum chemical parameters mean that the adsorption strengths of the molecules would be mostly determined by molecular size parameters rather than electronic structure parameters.

The local re-activities of each molecule was analyzed by means of the Fukui indices (FI) to assess reactive regions in terms of nucleophilic and electrophilic behaviour to distinguish each part of the molecule on the basis of its distinct chemical behavior due to different functional groups or substituents. The F^- measures

reactivity with respect to electrophilic attack or the propensity of the molecule to release electrons, whereas F^+ is a measure of reactivity relating to nucleophilic attack or tendency of the molecule attract electrons. The obtained values were presented in Table 2. In the electrophilic (F^-), citric, tartaric and malic acids have their highest Mulliken and Hirshfeld charges on O(20), O(13) and O(10) respectively. While for the nucleophilic (F^+), citric acid on C(12) and O(13), tartaric acid on C(1) and O(2) and malic acid on C(12) and O(13) respectively. The similarities in quantum chemical parameters mean that the adsorption strengths of the molecules would mostly be determined by molecular size parameters rather than electronic structure parameters alone [41,47].

Table 2 present results of some other electronic and structural quantum chemical parameters of the studied hydroxycarboxylic acid molecules. These include their; ionization potential, electron affinity absolute (global) hardness, global softness, absolute electronegativities and fraction of electron transferred respectively. The number of electrons transferred from the molecule to metal ΔN, where aluminium is considered as Lewis acid according to HSAB concept [41, 47]. The difference in electronegativity between the inhibitor and the aluminium drives the electron transfer, and the sum of the hardness parameters acts as a resistance. In order to calculate the fraction of electrons transferred, a theoretical value for the electronegativity of bulk aluminium was used χ_{Al} = 5.6 eV, and a global hardness of η_{Al} = 0, by assuming that for a metallic bulk I = A [41, 48], because they are softer than the neutral metallic atoms. From table 2, the fraction of electron transferred was found to be highest in tartaric acid than in others. The trend observed was: tartaric acid >citric acid = malic acid. Sastri and Perumareddi [41, 49] reported that if ΔN is less than 3.6, inhibition efficiency increases with increasing values of the electron donating ability of the molecules, while values of ΔN greater than 3.6 indicate a decrease in inhibition efficiency with increase in electron donating ability of the inhibitor. The earlier case is found to be applicable to all the studied molecules since their ΔN values are all less than 3.6.

Adsorption of the each hydroxycarboxylic acid molecules on the metal surface was analyzed at a molecular level by MD simulations, using Forcite quench MD to sample many different low-energy configurations and identify the low-energy minima [41, 50-51]. Calculations were carried out using the COMPASS force field and the Smart algorithm in a simulation box 30 Å × 25 Å × 29 Å with periodic boundary conditions to model a representative part of the interface, devoid of arbitrary boundary effects. The box composed of the Al slab, cleaved along the (1 1 0) plane, and a vacuum layer of 20 Å height. The geometry of the bottom layer of the slab was constrained to the bulk positions, whereas other degrees of freedom were relaxed before optimizing the Al (1 1 0) surface, which was subsequently enlarged into a 9 × 7 supercell. The molecules were adsorbed on one side of the slab. Temperature was fixed at 350 K, with NVE (microcanonical) ensemble, with a time step of 1 fs and simulation time 5 ps. The system was quenched every 250 steps.

Optimized structures of the hydroxycarboxylic acids and the Al surface were used for the simulation.

Figure 5 shows representative snapshots of the top view (inset) of the lowest energy adsorption configurations for single molecules of the inhibitors respectively, on the Al (1 1 0) surface from the simulations. Each molecule can be seen to maintain a flat-lying adsorption orientation on the Al surface, as expected from the delocalization of the electron density (figures 2-4) all around the molecules. This orientation maximizes contact with the metal surface and hence may augment high degree of surface coverage. The adsorption energy (*E*ads) for the most stable configuration of the constituents on the Al (1 1 0) surface was computed using the relationship in equation 12.

The total energies were calculated by averaging the energies of the three most stable representative adsorption configurations. The obtained *E*ads values, −28.384 kcalmol^{-1} for citric acid, −19.628 kcalmol^{-1} for tartaric acid, −19.982 kcalmol^{-1} for malic acid which are all negative and of relatively low magnitude, suggesting unstable adsorption structures which may lead to low inhibition. The trend in *E*ads corresponds to the trend in molecular size and number of –OH groups showing that the larger molecules are more strongly adsorbed on the Al metal surface. This low affinity of the inhibitors for the aluminium surface may account for low corrosion inhibition efficacy of the molecules expected to be observed experimentally. However, the magnitudes of the calculated binding energies were all less than 100 kcal mol^{-1} (Table 3), this is despite the fact that the simulations did not

take into consideration the specific covalent interactions between the molecules and the aluminium surface. Values less than or equal to 100 kcal mol^{-1} has been reported by John and Joseph [47] to be in the range of physisorptive interactions. It has also been reported that the more negative the binding energy of the inhibitor-metal surface is, the better the adsorption of the inhibitor onto the metal surface and subsequently the higher the inhibition [47, 52]. It can be observed from table 3 that a trend could be inferred in terms of inhibition efficiencies of the inhibitors in respect of their binding energies as follows: citric acid > malic acid > tartaric acid.

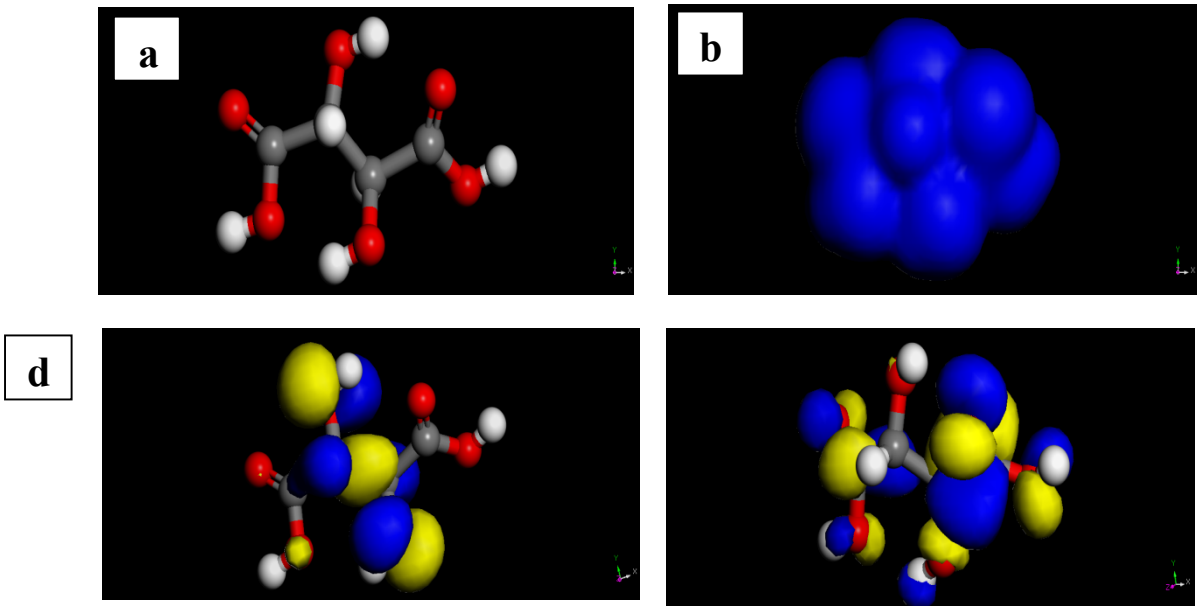

Figure 2: Electronic and Structural Properties of Tartaric Acid: a) Geometry Optimized b) Total Electron Density c) Highest Occupied Molecular Orbital d) Lowest Unoccupied Molecular Orbital

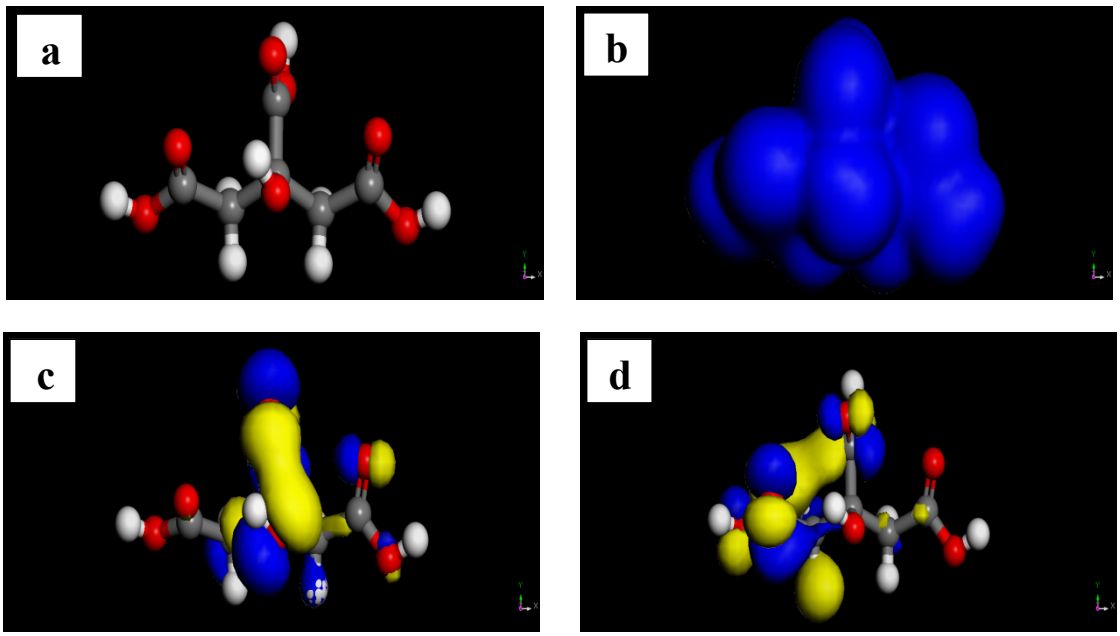

Figure 3: Electronic and Structural Properties of Citric Acid: a) Geometry Optimized b) Total Electron Density c) Highest Occupied Molecular Orbital d) Lowest Unoccupied Molecular Orbital

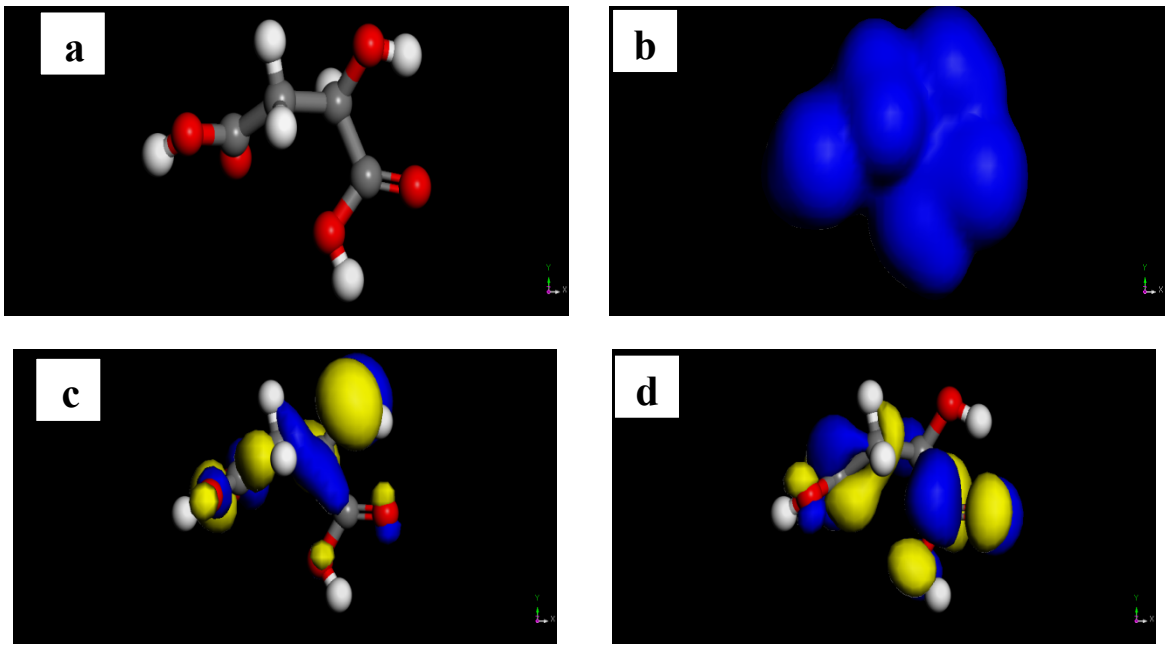

Figure 4: Electronic and Structural Properties of Malic Acid: a) Geometry Optimized b) Total Electron Density c) Highest Occupied Molecular Orbital d) Lowest Unoccupied Molecular Orbital

Table 1: Computed Quantum Chemical Parameters (Electronic and Structural) of the Studied Inhibitor Molecules

	Inhibitors		
Properties	**Citric Acid**	**Tartaric Acid**	**Malic Acid**
HOMO (at orbital number)	50	39	35
LUMO (at orbital number)	51	40	36
EHOMO (eV)	-6.721	-6.560	-6.622
ELUMO (eV)	-1.721	-1.818	-2.070
ΔE (eV)	5.000	4.742	4.552
Dipole Moment (Debye)	3.720	2.590	2.460
Molecular Weight (g/mol)	192.123	150.086	134.087
Ionization Potential (I) (eV)	6.721	6.560	6.622
Electron Affinity (A) (eV)	1.721	1.818	2.070
Global Hardness (**η**)	2.500	2.371	2.276
Global Softness (**σ**)	0.400	0.422	0.439
Absolute Electronegativity (**χ**)	4.221	4.189	4.346
Fractions of Electrons Transferred (ΔN)	0.276	0.298	0.276

Table 2: Calculated Fukui Indices for the Studied Inhibitor Molecules

	Electrophilic (F^-)				Nucleophilic (F^+)			
	Mulliken		Hirshfeld		Mulliken		Hirshfeld	
Molecule	**Atom**	**Value**	**Atom**	**Value**	**Atom**	**Value**	**Atom**	**Value**
Citric Acid	O(20)	0.188	O(20)	0.158	C(12)	0.143	O(13)	0.131
Tartaric Acid	O(13)	0.255	O(13)	0.227	C(1)	0.178	O(2)	0.161
Malic Acid	O(10)	0.298	O(10)	0.269	C(12)	0.193	O(13)	0.178

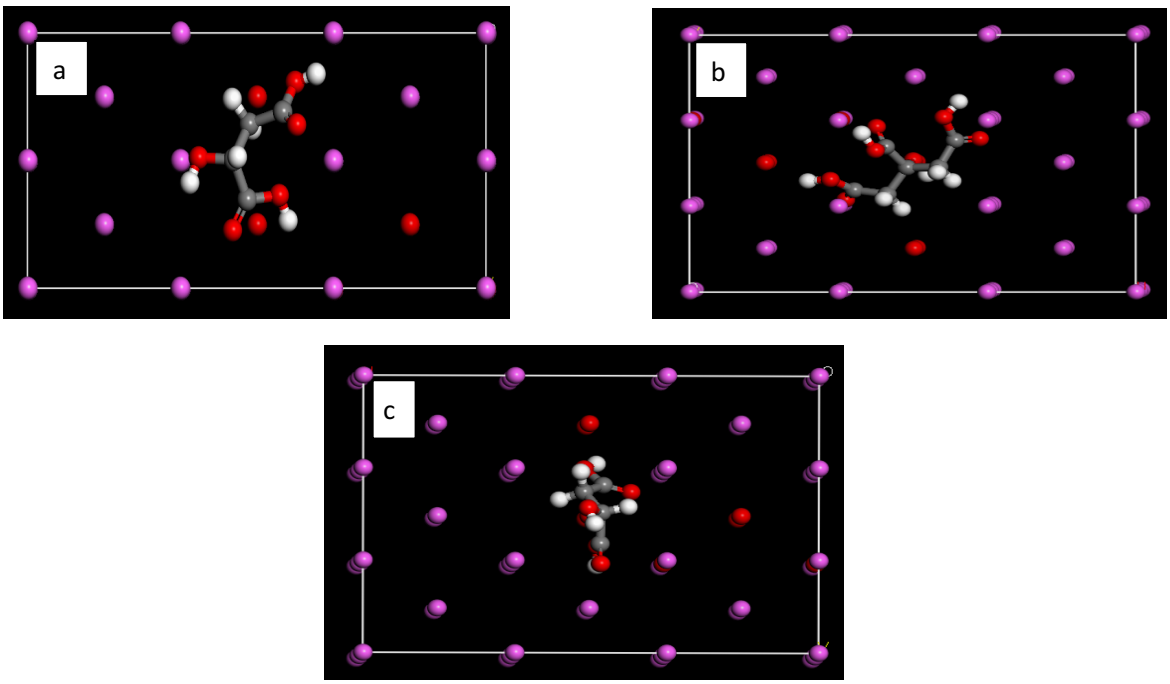

Figure 5: Adsorption of Single a) Tartaric Acid b) Citric Acid c) Malic Acid Molecules on Aluminium (110) Surface

Table 3: Calculated Adsorption Parameters for the Interaction of the Studied Molecules with the Al(110) Surface Using Forcite Quench Dynamics

	Molecule		
Properties	**Citric Acid**	**Tartaric Acid**	**Malic Acid**
Total Potential Energy (kcal/mol)	-78.458±0.734	-32.678±0.352	-32.609±0.261
Energy of Molecule (kcal/mol)	-50.074±3.457	-13.059±5.696	-12.627±6.035
Energy of Al (110) Surface (kcal/mol)	0.000±0.000	0.000±0.000	0.000±0.000
Adsorption Energy (kcal/mol)	-28.384±4.115	-19.628±5.477	-19.982±5.774

Conclusion

This work showed that the hydroxycarboxylic acids molecules can inhibit the corrosion of aluminum metal surface. There is a direct relation between adsorption energy of these compounds and their molecular weight; as molecular weight increases, the adsorption energy also increases. Quantum chemical calculations and Fukui indices showed that the molecules may adsorb to the Al metal surface trough the –OH groups rather than the –COOH groups. The separation energy ΔE, which is a function of reactivity, is correlated with the adsorption efficiency of the studied inhibitors. As ΔE decreases, the reactivity of the inhibitor towards the metal surface increases. The molecular dynamics simulation results showed that all inhibitors could adsorb on the aluminum metal surface in the same manner showing a great similarity in their structure.

References

1. M. K. Awad, *Canadian Journal of Chemistry,* 91 (2013) 283–291.
2. N. O. Eddy, P. O. Ameh, N. B. Essien, *Journal of Taibah University for Science*, 12(5)(2018) 545-556.
3. H. Ashassi-Sorkhabi, Z. Ghasemi, D. Seifzadeh, *Appl. Surf. Sci.* (2005) 408-418.
4. H. Lgaz, R. Salghi, A. Chaouiki, Shubhalaxmi, S. Jodeh, K. S. Bhat, *Cogent Engineering* 5 (2018) 1441585.
5. L. Garrigues, N. Pebere, F. Dabosi, *Electrochim. Acta,* 41(1996**)** 1209-1220.
6. Z. Szklarska-Smialowska, *Corros. Sci.* 41 (1999) 1743 - 1751.
7. I. B. Obot, N. O. Obi-Egbedi, *Colloids and Surfaces A: Physicochem. Eng. Aspects* (2008) 330- 207.
8. A. A. Khadom, *Journal of Materials and Environmental Sciences* 8(4)(2017) 1153-1160

9. T. V. Kumar, J. Makangara, C. Laxmikanth, N. S. Babu, *International Journal of Computational and Theoretical Chemistry* 4(1) 20161-6.
10. M. S. Masoud, M. K. Awad, M. A. Shaker, M. M. T. El-Tahawy, *Corros. Sci.,* 52 (2010) 2387-2394.
11. H.J. Henriquez-Roman, L. Padilla-Campos, M.A. Paez, J.H. Zagal, M.A. Rubio, C.M. Rangel, J. ostamagna, G. Cardenas-Jiron, *J. Mol. Struct. (THEOCHEM),* 757 (2005) 1-12.
12. N. Khalil, *Electrochim. Acta,* 48 (2003) 2635-2642.
13. M. Behpour, S. M. Ghoreishi, N. Soltani, M. Salavati-Niasari, M. Hamadanian, A. Gandomi, *Corros. Sci.,* 50 (2008) 2172-2179.
14. M. K. Awad, R. M. Issa, F. M. Atlam, *Mater. Corros.* 60 (2009) 813-819.
15. M. K. Awad, *J. Electroanal. Chem.* 567 (2004) 219-227.
16. I. N. Levine, *Quantum Chemistry*; Prentice Hall: Upper Saddle River, NJ, (1991).
17. C. Verma, M. A. Quraishi, K. Kluza, M. Makowska-Janusik, L. O. Olasunkanmi, E. E. Ebenso, *Scientific Reports*, 7 (2017) 44432.
18. C. D. D. Sundari, S. Setiadji, M. A. Ramdhani, A. L. Ivansyah, N. I. T. Widhiasari, The 2nd Annual Applied Science and Engineering Conference (AASEC 2017) IOP Publishing IOP Conf. Series: *Materials Science and Engineering*, 288 (2018) 012033.
19. H. Serrara, M. Laroujb, H. L. Gazb, Z. Benzekria, A. Zarguila, H. Essebaaid, S. Boukhrisa,H. Ouddab, R. Salghic, A. Hassikoua, A. Souizia, *Portugaliae Electrochimica Acta* 36(1) (2018) 35-52.
20. T. A. Salman, K. F. Al-Azawi, I. M. Mohammed, S. B. Al-Baghdadi, A. A. Al-Amiery, T. S. Gaaz, A. A. Kadhum, *Results in Physics* 10 (2018) 291-296.
21. K. F. Khaled, M. M. Al-Qahtani, *Materials Chemistry and Physics*, 113 (2009) 150–158.
22. A. Popova, M. Christov, T. Deligeorgiev, *Corrosion*, 59 (2003) 756-760.
23. A. Popova, M. Christov, S. Raicheva, E. Sokolova, *Corros. Sci*., 46 (2004) 1333-1345.
24. A. Popova, M. Christov, *Corros. Sci.* 48 (2004) 33-58.
25. I. B. Obot, N. O. Obi-Egbedi, E. E. Ebenso, A. S. Afolabi, E. E. Oguzie, *Research on Chemical Intermediates*, 39 (2013) 1927-1948.
26. S. A. Abd El-Maksoud, *Corros. Sci*., 44 (2002) 803-814.
27. M. Ajmal, A. S. Mideen, M. A. Quraishi, *Corros. Sci*., 36 (1994) 79-83.
28. C. D. Bain, E. B. Throughton, Y. T. Tao, J. Evall, G. M. Whiteside, J. G. Nuzzo, *J. Am. Soc.,* 111 (1989) 321-331.
29. W. Yang, R. G. Parr, Proc. Natl. Acad. Sci. USA 82, 6723, (1985).
30. W. Yang, W. J. Mortier, *J. Am. Chem. Soc.*, 108 (1986) 5708-5711.
31. C. Vermaa, M. A. Quraishia, L.O. Olasunkanmib, E. E. Ebenso, *Royal Society of Chemistry (Advances)*, 2018 1-52.
32. V.M. Udowo, I. E. Uwah, F. E. Daniel, F. Abeng, S. Ivara, *Journal of Physical Chemistry & Biophysics* 7:3 (2017) 1-6.
33. K. Rasheeda, D. P. Vijaya, P. A. Alva, Krishnaprasad, S. Samshuddin, *Int. J. Corros. Scale Inhib*., 7(1) 2018 48–61.
34. N. O. Obi-Egbedi, N. D. Ojo, *Journal of Science Research*, 14 (2015) 50-56.
35. H. Zhao, X. Zhang, L. Ji, H. Hu, Q. Li, Corrosion Science 2 (2014) 11-23.
36. A. Mishra, C. Verma, V. Srivastava, H. Lgaz, M. A. Quraishi, E. E. Ebenso,M. Chung, *Journal of Bio- and Tribo-Corrosion* (2018) 4:32.
37. K. F. Khaled, M. A. Amin, *Corros. Sci.*, 51 (2009) 2553-2568.
38. G. Bereket, C. Ogretir, A. Yurt, *J. Mol. Struct. (Theochem)*, 571 (2001) 13.
39. B. Delley, *The Journal of Chemical Physics,* 92 (1990) 508–517.
40. B. Delley, *The Journal of Chemical Physics,* 113 (2000) 7756–7764.
41. A. M. Ayuba, A. Uzairu, H. Abba, G. A. Shallangwa, Morrocan Journal of Chemistry, 6(1) (2018) 160-172.
42. K. F. Khaled, *Corrosion Science,* 52 (2010) 3225–3234.
43. S. Martinez, *Materials Chemistry and Physics,* 77 (2003) 97–102.
44. J. Fu, S. Li, L. Cao, Y. Wang, L. Yan, L. Lu, *Journal of Materials Science,* 45 (2010) 979–986.
45. J. Fu, S. Li, Y. Wang, X. Liu, L. Lu, *Journal of Materials Science,* 46 (2011) 3550–3559.
46. L. M. Rodriguez-Valdez, A. Martinez-Villafane, D. Glossman-Mitnik, D. Glossman-Mitnik, *Journal of Molecular Structure: THEOCHEM,* 713 (2005) 65–70.
47. S. John, A. Joseph, *Materials and Corrosion*, 64(7) (2013) 625-632.
48. P. Zhao, Q. Liang, Y. Li, *Applied Surface Science,* 252(5) (2005) 1596-1607.
49. V. S. Sastri, J. R. Perumareddi, *Corrosion,* 53(8) (1997) 617-622.
50. C. J. Casewit, K. S. Colwell, A. K. Rappe, *Journal of the American Chemical Society,* 114 (1992)10035–10046.
51. C. J. Casewit, K. S. Colwell, A. K. Rappe, *Journal of the American Chemical Society,* 114 (1992) 10046–10053.
52. F. E. Awe, S. O. Idris, M. Abdulwahab, E. E. Oguzie, *Cogent Chemistry*, 1 (2015) 1-14.